# Efficient and Robust Data Collection Using Compact Micro Hardware, Distributed Bus Architectures and Optimizing Software

Savio Chau [1], Farrokh Vatan[2], Vincent Randolph [3], and Edmund C. Baroth [4]
*Jet Propulsion Laboratory, California Institute of Technology, Pasadena, CA, 90019*

**Future In-Space propulsion systems for exploration programs will invariably require data collection from a large number of sensors. Consider the sensors needed for monitoring several vehicle systems' states of health, including the collection of structural health data, over a large area. This would include the fuel tanks, habitat structure, and science containment of systems required for Lunar, Mars, or deep space exploration. Such a system would consist of several hundred or even thousands of sensors. Conventional avionics system design will require these sensors to be connected to a few Remote Health Units (RHU), which are connected to robust, micro flight computers through a serial bus. This results in a large mass of cabling and unacceptable weight. This paper first gives a survey of several techniques that may reduce the cabling mass for sensors. These techniques can be categorized into four classes: power line communication, serial sensor buses, compound serial buses, and wireless network. The power line communication approach uses the power line to carry both power and data, so that the conventional data lines can be eliminated. The serial sensor bus approach reduces most of the cabling by connecting all the sensors with a single (or redundant) serial bus. Many standard buses for industrial control and sensor buses can support several hundreds of nodes, however, have not been space qualified. Conventional avionics serial buses such as the Mil-Std-1553B bus and IEEE 1394a are space qualified but can support only a limited number of nodes. The third approach is to combine avionics buses to increase their addressability. The reliability, EMI/EMC, and flight qualification issues of wireless networks have to be addressed. Several wireless networks such as the IEEE 802.11 and Ultra Wide Band are surveyed in this paper. The placement of sensors can also affect cable mass. Excessive sensors increase the number of cables unnecessarily. Insufficient number of sensors may not provide adequate coverage of the system. This paper also discusses an optimal technique to place and validate sensors.**

## I. Introduction

Cabling has always been a major problem for space systems. In a typical spacecraft, cables take up about 7% to 10% of the dry mass. For small-unmanned space probes, this might be an acceptable burden. However, this will not be acceptable for long duration crewed missions such as Mars exploration. If that mass could be saved, the astronauts would have more food, fuel, or other supplies to endure the long trip.

In a conventional space system, the most cable intensive area in a spacecraft is probably the wiring to sensors. This is mainly because of the multitude of sensors, but it is also because of the centralized point-to-point architecture of these systems. Therefore, the first step toward cable reduction is to eliminate the large number of cables required by the centralized point-to-point architecture. There are two general approaches: distributed architecture and wireless network. This paper provides a survey of the technologies in these two areas. Careful trade studies have to be performed among the technologies for specific system design.

## II. Cable Reduction by Distributed Architecture

A distributed architecture consists of many "nodes" that are connected by a network. Each of these nodes has some level of intelligence that can collect and process data locally. If the data are collected locally, the cables from each node to the sensors are much shorter than the centralized architecture. Furthermore, since each node can process data locally, the information exchanged between nodes is much less frequent, so that a serial bus is sufficient to handle the data traffic between nodes.

---

[1] Principal Engineer, Autonomous Systems Architecture & Program Development Section, JPL Mail-Stop 198-219
[2] Senior Engineer, Flight Software & Data Systems Section, JPL Mail-Stop 126-157
[3] Senior Engineer, Flight System Electronics Section, JPL Mail-Stop 156-142
[4] Principal, Autonomous Systems Architecture & Program Development Section, JPL Mail-Stop 156-142

This paper has identified three approaches to implement the distributed architecture for cable reduction.

1. Power line communication
2. Serial sensor buses
3. Compound serial buses

The important design factors of distributed architectures in cable reduction are complexity of interconnections, throughput (i.e., bandwidth), and number of nodes accommodated by the network.

## A. Power Line Communication

This approach uses the power line as communication network to pass messages between nodes. This technology has been developed by the home network industry. Examples include LonWorks[1] and HomePlug.[2] Both of these networks can use the power line as physical media and power outlet as data port. (Note: both protocols can be used on other media such as twist wire also.) The data rate of LonWorks is 5.4 Kbps and the HomePlug is 6 Mbps (field tests gave rates from 1.6 to 5.3 Mbps at the application level).

### *1. LonWorks*

LonWorks sends signals on the power line with carrier frequency in the range of 110 kHz to 140 kHz.[3] LonWorks transceiver incorporates a dual carrier frequency capability that allows it to communicate with other LonWorks nodes, even if noise is blocking its primary communication frequency range. If impairments prevent communication in the primary frequency (132 kHz), a LonWorks node can automatically switch to a secondary carrier frequency (115 kHz) to complete the transaction.

The physical layer protocol of LonWorks is shown in Figure 1. Data are sent as 32-byte packets. Most of the data packets are sent with unacknowledged service, with a request/response packet sent every six packets. These five unacknowledged packets and the sixth request/response packet constitute a data window. The Request packet contains the request from the sender and the Response packet from a receiver contains the number of last packet successfully received incremented by one. For example, if a sender sends 5 packets to a receiver and all 5 packets are received successfully, then the receiver will return a value of 5 + 1 = 6 in the Response packet.

The application layer of LonWorks has are 32 predefined commands which include on, off, dim, play, rewind, fast forward, pause, skip, and temperature up or down one degree. LonWorks standard allows for more than 32,000 devices in a network, with addresses preset in the factory or alterable at time of installation.

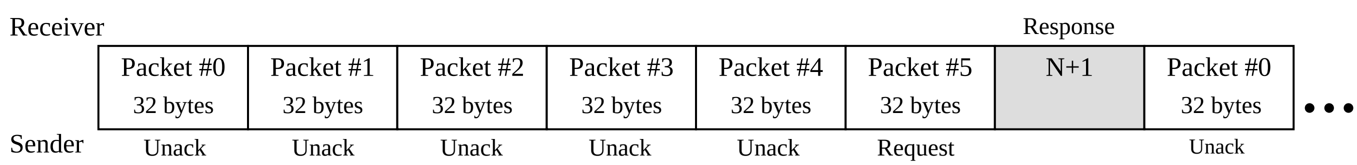


**Figure 1. LonWorks Protocol**

### *2. HomePlug*

The physical layer frame format of HomePlug is shown in Figure 2. The HomePlug protocol is based on orthogonal frequency division multiplexing (OFDM) and carrier sense multiple access with collision avoidance (CSMA/CA), along with its changes to allow prioritized channel access. The basic idea of OFDM is to divide the available spectrum into several narrowband, low data rate subcarriers. To obtain high spectral efficiency the frequency response of the subcarriers are overlapping and orthogonal, hence the name OFDM. The property of orthogonality is a result of choosing the carrier spacing equal to the inverse of the bit rate on each carrier. The practical consequence of orthogonality is that the data stream that modulates a narrowband of subcarrier is not impacted by the data stream modulating any other carrier. Therefore, multiple bit streams can be same simultaneously.

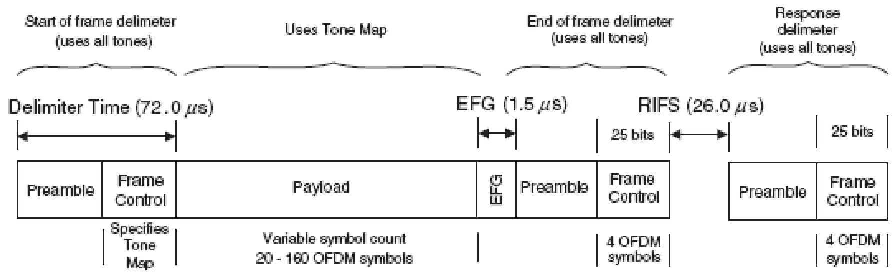


**Figure 2. HomePlug Physical Layer Frame Format**

The advantage of using power line communication for distributed architecture is no need to have data cables as the power lines carry communication. The disadvantage is power line medium is a harsh environment for communication. The channel between any two outlets in a network has the transfer function of an extremely complicated transmission line network with many stubs having terminating loads of various impedances. Such a network has an amplitude and phase response that varies widely with frequency. In addition, neither the LonWorks nor the HomePlug has been flight qualified.

The power line communications approach has some technically challenging problems. First, this approach is originally designed to use 50-60Hz power in the home, while most of the power distribution networks on spacecraft are DC. Second, the frequency response can also vary with time as the load on the network changes. Third, power line networks are also affected by interference. Noise generated by the equipment on the spacecraft can reduce the reliability of communication signals. Due to high attenuation over the power line, the noise is also location dependent. These problems can be overcome by using robust transmission technique combined with sophisticated forward error correction, error detection, data interleaving, and automatic repeat request. However, their EMI/EMC effects on other spacecraft equipment have not been fully studied.

## B. Serial Sensor Bus

### *1. FieldBus*

There is a large family of serial buses that has been used for industrial control under the name of Fieldbus. Examples of Fieldbus including the ModBus®, DeviceNet®, AS-interface®, Profibus®, Foundation Fieldbus®. These buses have similar but slightly different designs. A common feature of these buses is that they use a twisted pair for communications and two wires for power. Hence, any one of these buses can be used as a serial bus to connection a large number of sensors (e.g., the ModBus can connect 10 networks of 800 nodes in a system.) A summary of these buses can be found in Table 1.[4]

| **Network Protocol Overview** | **ModBus®** | **ModBus Direct** | **DeviceNet®** | **AS-interface®** | **Profibus®** | **Foundation Fieldbus** |
|---|---|---|---|---|---|---|
| **Physical Media** | Twisted pair for communications, two wires for power | Twisted pair for communications two wires for power | Twisted pair for communications two wires for power | Two wire cable (communications & power) | Twisted pair for communications, two wires for power | |
| **Maximum Distance** | 3000ft. | 3000ft. | 1600ft. | 300ft.<br>900ft. with repeater | 1000 m | 3000ft. |
| **Maximum I/O Points per System** | 800 / network<br>8000 / system | 256 / network plus optional | 504 / network plus optional | 248 / network<br>248 / system | 1008 / system | 256/network plus optional |
| **Current Consumption** | 60 mA + 20-25 mA/coil | 60 mA + 20-25 mA/coil | 50 mA | 80 mA | 120 mA | 60 mA + 20-25 mA/coil |
| **Interface Capability** | All PLC's & DCS w/ModBus Port | All PLC's & DCS w/ModBus, Port | Allen-Bradley, Omron, GE, Siemens | All PLC's & DCS w/ModBus, DeviceNet, ProfiBus Port | All PLC's & DCS supporting the Profibus protocol | All PLC's & DCS w/ModBus, Port |
| **Communications Method** | Master/slave with cyclic polling | Master/slave with cyclic polling | Master/slave multimaster, peer-to-peer | Master/slave with cyclic polling | Master/slave with cyclic polling | Master/slave with cyclic polling |

| | | | | | | |
|---|---|---|---|---|---|---|
| **Error Checking** | CRC check | CDC check | CRC check | Control sum, parity | CRC check | CDC check |
| **Network Topology** | Closed loop bus | Trunkline / dropline with branching | Trunkline / dropline with branching | Bus, tree, star | Trunkline/dropline with branching | Trunkline/dropline with branching |
| **Transmission Speed** | 9.6 kbps | 9.6kps, 19.2kps | 125 kbps, 250 kbps, 500 kbps | 167 kbps | 9.6 kbps to 12 mbps | 9.6kps, 19.2kps |
| **Redundancy** | Yes | No | No | No | No | No |
| **Valves Specific Diagnostics** | Yes | Yes | Yes | No | Consult Factory | Yes |

**Table 1. Summary of Some FieldBuses**

*2. IEEE 1451*

Another sensor bus standard is the IEEE 1451[5] The IEEE 1451 is actually a family of Smart Transducer Interface Standards describing a set of open, common, network-independent communication interfaces for connecting transducers (sensors or actuators) to microprocessors, instrumentation systems, and control/field networks. The key feature of these standards is the definition of a Transducer Electronic Data Sheet (TEDS). The TEDS is a memory device attached to the transducer, which stores transducer identification, calibration, correction data, and manufacture-related information. An example of a TEDS for an accelerometer is shown in Figure 3. The goal of 1451 is to allow the access of transducer data through a common set of interfaces whether the transducers are connected to systems or networks via a wired or wireless means. The standards in the IEEE 1451 family are listed below.

| | | |
|---|---|---|
| **Basic TEDS** | Manufacturer ID | 43 (Acme Accelerometer Company) |
| | Model Number | 7115 |
| | Version Letter | B |
| | Serial Number | X001891 |
| **Standard and Extended TEDS** (fields will vary according to transducer type) | Calibration Date | Jan 29, 2000 |
| | Sensitivity @ ref. condition (S ref) | 1.0094E+03 mV/g |
| | Physical measurement range | ± 50 g |
| | Electrical output range | ± 5 V |
| | Reference frequency (f ref) | 100.0 Hz |
| | Quality factor @ fref (Q) | 300 E-3 |
| | Temperature coefficient | -0.48 %/°C |
| | Reference temperature (T ref) | 23 °C |
| | Sensitivity direction (x,y,z) | x |
| **User Area** | Sensor Location | Strut 3A |
| | Calibration due date | April 15, 2002 |

**Figure 3. Example TEDS of an Accelerometer**

1. **IEEE P1451.0** [Note 1]**:** defines a set of common operations and Transducer Electronic Data Sheet (TEDS) for the family of IEEE 1451 smart transducer standards. The functionality is independent of the physical communications media between the transducer and Network Capable Application Processor (NCAP). This makes it easy to add other proposed 1451.X physical layers to the family.
2. **IEEE 1451.1** [Note 3]**:** defined a common object model and programming paradigm for smart transducer systems. This software runs on the NCAP and interacts with transducers through the other 1451.X physical layers standards. Communications between groups of NCAPs and higher-level systems are supported in a network neutral manner.
3. **IEEE 1451.2** [Note 3]**:** defined a transducers-to-NCAP interface and TEDS for a point-to-point configuration. Transducers are part of a Smart Transducer Interface Module (STIM). The original standard describes a communication layer based on SPI standard interface with additional hardware lines for flow control and timing. This standard is being revised to support two popular serial interfaces: UART and USB.
4. **IEEE 1451.3** [Note 3]**:** defined a transducer-to-NCAP interface and TEDS for multi-drop transducers using the Home Phoneline Networking Alliance (HPNA) communication protocol. It allows many transducers to be arrayed as nodes, on a multi-drop transducer network, sharing a common pair of wires.

5. **IEEE 1451.4** Note 2**:** defined a mixed-mode interface for analog transducers with analog and digital operating modes. A TEDS was added to a traditional two-wire, constant current excited sensor containing a FET amplifier. The TEDS model was also refined to allow a bare minimum of pertinent data to be stored in a physically small memory device, as required by tiny sensors. Addition to the TEDS was defined for other sensor types as well.
6. **IEEE P1451.5** Note 1**:** defines a transducer-to-NCAP interface and TEDS for wireless transducers. Wireless standards such as 802.11 (WiFi), 802.15.1 (Bluetooth), 802.15.4 (ZigBee) are being considered as some of the physical interfaces.
7. **IEEE P1451.6** Note 1**:** defines a transducer-to-NCAP interface and TEDS using the high-speed CANopen network interface. Both intrinsically safe and non-intrinsically safe applications are being supported. It defines a mapping of the 1451 TEDS to the CANopen dictionary entries as well as communication messages, process data, configuration parameter, and diagnosis information. It adopts the CANopen device profile for measuring devices and closed-loop controllers.

Note 1**:** The proposed standard is being developed.
Note 2**:** The proposed standard has been balloted and is awaiting publication.
Note 3**:** The standard is in publication and can be acquired at the IEEE.org web site.

In terms of cable reduction, the IEEE 1451.3[6] is probably is the best option because it defines a digital multi-drop sensor interface with only a small number of connections. Figure 4 shows the connectivity diagram of an IEEE 1451.3 system. In this representation, there are two conductors between the *Transducer Bus Controller* (TBC) and the *Transducer Bus Interface Module* (TBIMs). These two conductors carry both the power and the signals to implement the interface. In some cases, more power is required for a particular TBIM than is supplied over the bus and an auxiliary power source may be required.

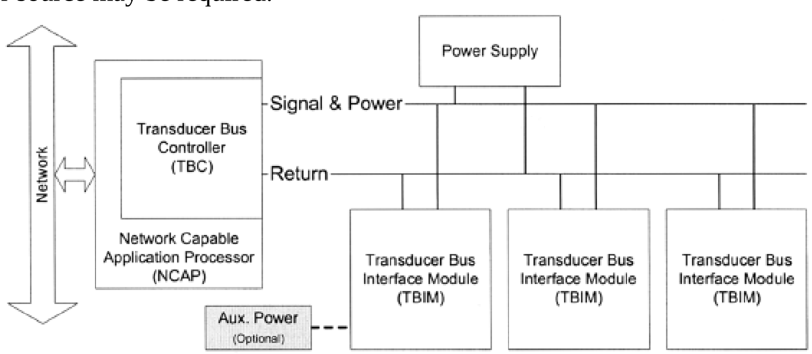


**Figure 4. Electrical Connectivity of IEEE 1451.3 Sensor Bus**

The IEEE 1451.3 has a sine-wave synchronization signal that is provided to assure that all TBIMs on a bus have access to a clock running at the same frequency. The TBIM communication is implemented using the HomePNA communications standard. Combining power, synchronization, and communication signals on a single pair of conductors is accomplished by separating them into separate frequency spectra. The frequency of the synchronization signal is 2.0MHz and the communications lies between 4.75MHz and 9.25MHz, so all of them may be transmitted on the same wires without them interfering with each other. Appropriate filters are required to separate the signals at the receiver.

The IEEE 1451.3 has a 16-bit address, eight of which are used for node address (TBC or TBIM) and the other eight bits are used as channel numbers within each node. The IEEE 1452.3 can therefore support a maximum network size of one TBC and 254 TBIM (address 0 is used for broadcast); each TBIM can have 255 Transducer Channels. That equates to over 60,000 smart sensors over a pair of conductors.

It should be noted that neither the FieldBus nor the IEEE 1451.3 has been flight qualified.

### C. Compound Serial Buses

While the power line communication approach and the serial sensor buses can reduce the cabling problem for space systems, none of them has been flight qualified. The most popular flight qualified data bus is the Mil-Std-1553B Bus. Unfortunately, the Mil-Std-1553B Bus can only accommodate 32 nodes and its raw data rate is only 1 Mbps. For a complex system that has thousands of nodes, tens of Mil-Std-1553B buses would be required. If all the

Mil-Std-1553B buses have to be centralized at the flight computer, then the cabling problem will not be completely solved.

To solve this problem, JPL has developed a compound serial bus architecture that uses an IEEE 1394A Bus as backbone bus to drive multiple Mil-Std-1553 Buses. This is shown as Figure 5. The IEEE 1394A Bus used for space applications has a data rate of 100 Mbps, which is two orders of magnitude faster than the 1 Mbps Mil-Std-155B Bus. JPL has also developed a fault tolerant bus architecture using two redundant IEEE 1394A Buses.[7] Both JPL and Northrop Grumman Corporation (NGC) has implemented the bus. The NGC chip set has recently been evaluated and is available for use in future space applications.[8]-

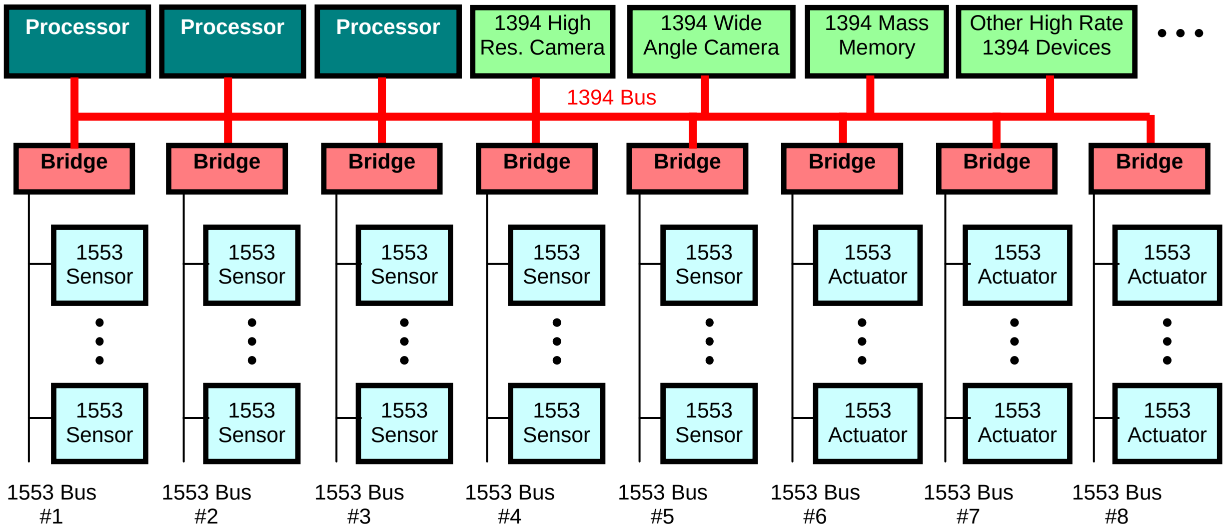


**Figure 5. Example of an IEEE 1394A/Mil-Std-1553B Compound Serial Bus Architecture**

A single IEEE 1394 Bus can address 64 nodes, so it can accommodate 64 Mil-Std-1553B Buses. Considering the bandwidth of each Mil-Std-1553B Bus is only 1 Mbps, the total bandwidth for 64 buses only occupies 64% of the IEEE 1394 Bus bandwidth and leaves a fairly comfortable margin for other applications. As each Mil-Std-1553B Bus can address 32 nodes, this bus architecture can accommodate up to 2048 nodes (i.e., 64 x 32 = 2048). Even if each node can handle only one sensor, this bus architecture will have capacity for 2048 sensors. If each node can handle multiple sensors, the capacity of the bus will be multiplied.

The IEEE 1394 Bus actually has a tree topology (not shown in Figure 5), with two pairs of twisted wire connection between each pair of nodes. The tree topology has a drawback that if a branch node fails, the bus will be partitioned. To solve this problem, JPL has developed a dual-redundant IEEE 1394A bus architecture using a "stack-tree" topology, in which any node in the system cannot be branch node in both buses. If a node fails, therefore, it can only partition one bus. The other bus loses a node but all the other nodes are still connected. In fact, the IEEE 1394A bus also has capability to activate or deactivate connection between nodes. Backup connections can be added to the bus architecture, so if a node or active connection fails, the backup connection can be activated to bypass the failed node or connection. This is illustrated in Figure 6.

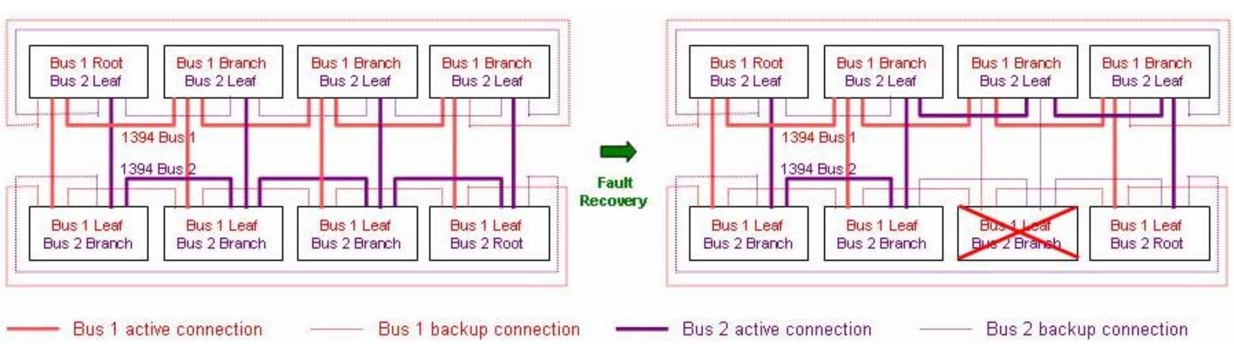


**Figure 6. Fault Tolerant IEEE 1394A Bus Architecture**

The Mil-Std-1553B and IEEE 1394A buses have been flight qualified. The bridge between the two buses has been jointly developed by JPL and the SEAKR Engineering Inc. However, the design of the bridge has not been flight qualified.

## III. Cable Reduction by Wireless Network

Wireless network can eliminate all cables except for the power cables. The complexity of interconnection is no longer a design factor. Other important design factors of wireless network are throughput (i.e., bandwidth), number of nodes accommodated by the network, multiple access capability, communication range, handling of self-interference due to multi-path, susceptibility to interference from external sources, and interference to telecommunication subsystem and other electronics. Although the application of a wireless network in space is more challenging then distributed architecture, a wireless network has other benefits such as natural electrical isolation and ease of system integration. So, wireless network for space is still a promising technology.

| | *UWB 802.15.3a TI Proposal ** | **802.11 Family** | | | **Bluetooth** | **802.16** |
|---|---|---|---|---|---|---|
| | | **802.11a** | **802.11b** | **802.11g** | | |
| **Frequency** | 3.168 GHz – 4.752 GHz | 5 GHz | 2.4 GHz | 2.4 GHz | 2.4 GHz | 10 - 66 GHz<br>2 - 11 GHz |
| **Max Data Rate** | 110 Mbps @ 10 m, 200 Mbps @ 4 m, *480 Mbps @ 2 m* | 54 Mbps | 11 Mbps | 54 Mbps | 720 Kbps | 70 Mbps |
| **Latency** | Not Available at this time | Not deter-ministic (due to Collision Avoidance) | Not deter-ministic (due to Collision Avoidance) | Not deter-ministic (due to Collision Avoidance) | Not deterministic (due to frequency hoping) | Controlled by Base Station |
| **Range** | 10 m | 50 m | 100 m | 100 m | <10m | 5 km |
| **Encoding Technique** | Time Modulation & Channel Coding | OFDM | DSSS | OFDM | FHSS | TDMA/OFDMA |
| **Multi-Access Approach** | Unknown at this time | CSMA/CA | CSMA/CA | CSMA/CA | FHSS | Point-to-Multipoint Central Base Station |
| **Network Control** | Not Available at this time | Peer-to-Peer but require Access Point | Peer-to-Peer but require Access Point | Peer-to-Peer but require Access Point | Centralized (master in piconet) | Centralized (master in Base Station) |
| **Duplex Method** | Not Available at this time | TDD: RTS → CTS → Data → ACK | TDD: RTS → CTS → Data → ACK | TDD: RTS → CTS → Data → ACK | TDD: 1 frame has 1 master slot (625 □s) and 1 slave slot. Multiple frame transaction allowed | TDD, FDD |
| **Number of Users/Channel** | Not Available at this time | 127 | 127 | 127 | 1 master, 7 active slaves, 200 inactive slaves / piconet | Variable |
| **Channel Spacing** | 503.25 MHz | OFDM: 20 MHz | DBPSK, DQPSK, CCK | OFDM: 20 MHz | 79 Channels, 1 MHz/channel | |

DSSS – Direct-Sequence Spread Spectrum; FHSS – Frequency Hopping Spread Spectrum;
TDMA – Time Division Multiple Access; OFDMA – Orthogonal Frequency Division Multiple Access;
CSMA/CA – Carrier Sensing Multiple Access / Collision Avoidance; ACK – Acknowledgment;
TDD – Time Division Duplex; FDD – Frequency Division Duplex; RTS – Request to Send; CTS – Clear to Send
DBPSK – Differential Bi-Phase Shift Keying (Information bits are identified by changes in phase of the carrier)
DQPSK – Differential Quadrature Phase Shift Keying

**Table 2. Characteristics of Modular Reconfigurable High Energy (MRHE) Wireless Network**

JPL has examined several wireless networks for the Modular Reconfigurable High Energy (MRHE) System project. The characteristics of these networks are summarized in Table 2. Brief descriptions of the networks are given in the following sections. It should be noticed that none of the wireless network surveyed here has been flight qualified. Much development efforts are required to mature the wireless network for space applications.

### A. IEEE 802.15.3A

The development of the IEEE 802.5.3a standard can be traced back to the IEEE 802.15 working group that develops personal area network standards for short distance wireless personal area networks (WPANs). Within the IEEE 802.15 working group, a sub-group call Task Group 3 has developed a standard (IEEE 802.15.3) to deliver data rates from 20 Mbps to 55 Mbps over short range (less than 10 meters) WPANs. There are many applications, however, that would require much higher data rate than 55 Mbps. In November 2001, an additional task group within IEEE 802.15, Task Group 3a, was formed to identify a higher speed physical layer alternative that could support data rates between 110 Mbps and 480 Mbps over short ranges of less than 10 meters.

In February of 2002, the FCC amended their Part 15 rules (concerning unlicensed radio devices) to include the operation of ultra wide band (UWB) devices without a license. The FCC defines UWB signals as having a fractional bandwidth of greater than 0.20 or a UWB bandwidth greater than 500 MHz. UWB bandwidth is defined as "the frequency band bounded by the points that are 10 dB below the highest radiated emission." The FCC ruling allows UWB communication devices to operate at low power (an EIRP of -41.3 dBm/MHz) in an unlicensed spectrum from 3.1 to 10.6 GHz (Figure 7). The low emission limits for UWB are to ensure that UWB devices do not cause harmful interference to (i.e., coexist with) "licensed services and other important radio operations." This development prompted many companies to consider UWB radio when proposing physical layers to IEEE 802.15.3a.

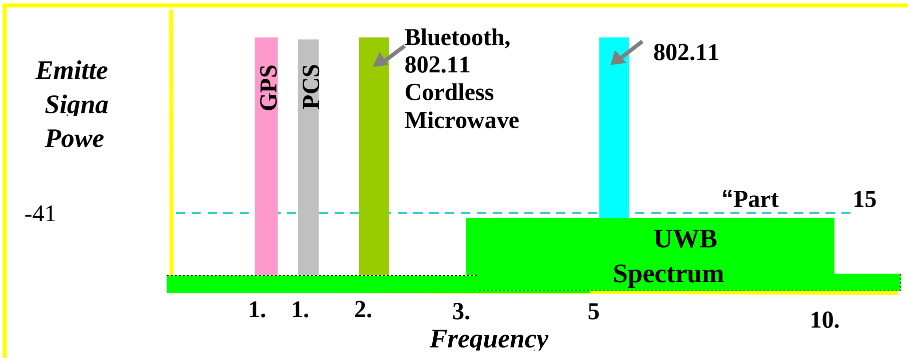


**Figure 7. FCC Ruling Permits UWB Spectrum Overlay**

The two major approaches being considered by IEEE 802.15.3a differ primarily with regard to their allocation of UWB spectrum.[9] Impulse Radio (IR), the traditional approach to UWB communication, involves the use of very short-duration pulses that occupy a single band of several GHz. Data is commonly modulated using pulse-position modulation (PPM); and multiple users could be supported using time-hopping or code-division multiple access (CDMA) scheme. An example of the pulse-position modulation with the CDMA scheme is shown in Figure 8.[10]

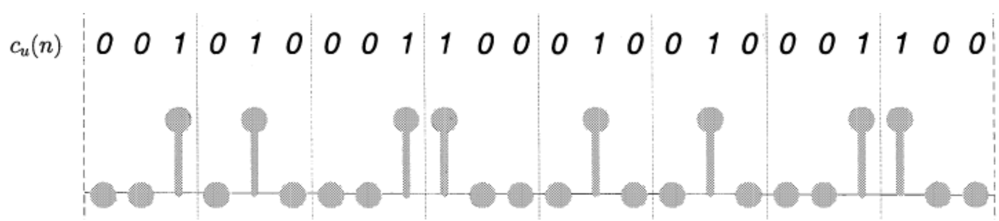


**Figure 8. Impulse Radio with CDMA Coding**

The other approach to UWB spectrum allocation is a multibanded system where the UWB frequency band from 3.1 - 10.6 GHz is divided into several smaller bands. Each of these bands must have a bandwidth greater than 500 MHz to comply with the FCC definition of UWB. Frequency hopping between these bands can be used to facilitate multiples access. Companies in the newly formed Multiband-OFDM coalition support this approach primarily because it has greater flexibility in adapting to the spectral regulation of different countries and avoids transmitting in already occupied bands. Figure 9 illustrates the division of the UWB spectrum into sub-bands

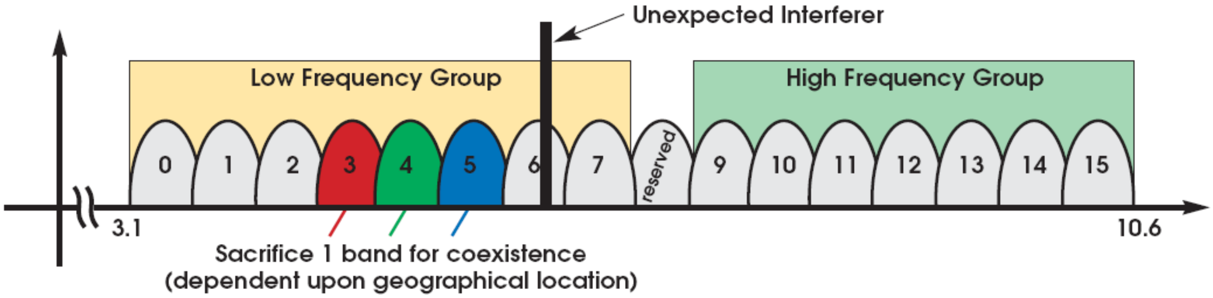


**Figure 9. Example of multiband spectrum allocation**

### B. IEEE 802.11

The IEEE 802.11 standard[11] places specifications on the parameters of both the physical (PHY) and medium access control (MAC) layers of the network. The PHY layer, which actually handles the transmission of data between nodes, can use either direct sequence spread spectrum, frequency hopping spread spectrum, or infrared (IR) pulse position modulation. IEEE 802.11 makes provisions for data rates of either 1 Mbps or 2 Mbps, and calls for operation in the 2.4 - 2.4835 GHz frequency band (in the case of spread-spectrum transmission), which is an unlicensed band for industrial, scientific, and medical (ISM) applications.

The MAC layer is a set of protocols that is responsible for maintaining order in the use of a shared medium. The 802.11 standard specifies a carrier sense multiple access with collision avoidance (CSMA/CA) protocol. In this protocol, when a node receives a packet to be transmitted, it first listens to ensure no other node is transmitting. If the channel is clear, it then transmits the packet. Otherwise, it chooses a random "backoff factor" which determines the amount of time the node must wait until it is allowed to transmit its packet. During periods in which the channel is clear, the transmitting node decrements its backoff counter. (When the channel is busy it does not decrement its backoff counter.) When the backoff counter reaches zero, the node transmits the packet. Since the probability that two nodes will choose the same backoff factor is small, collisions between packets are minimized. Collision detection, as is employed in Ethernet, cannot be used for the radio frequency transmissions of IEEE 802.11. The reason for this is that when a node is transmitting it cannot hear any other node in the system which may be transmitting, because its own signal will drown out any others arriving at the node.

Whenever a packet is to be transmitted, the transmitting node first sends out a short ready-to-send (RTS) packet containing information on the length of the packet. If the receiving node hears the RTS, it responds with a short clear-to-send (CTS) packet. After this exchange, the transmitting node sends its packet. When the packet is received successfully, as determined by a cyclic redundancy check (CRC), the receiving node transmits an acknowledgment (ACK) packet. This back-and-forth exchange is necessary to avoid the "hidden node" problem. To illustrate the hidden node problem, for example, node A can communicate with node B, and node B can communicate with node C. However, node A cannot communicate node C. Thus, for instance, although node A may sense the channel to be clear, node C may in fact be transmitting to node B. The protocol described above alerts node A that node B is busy, and hence it must wait before transmitting its packet.

### C. Bluetooth

*Bluetooth* wireless technology[12] is a short-range communications system intended to replace the cables connecting portable and/or fixed electronic devices. The key features of *Bluetooth* wireless technology are robustness, low power, and low cost. Many features of the core specification are optional, allowing product differentiation.

The *Bluetooth* core system consists of an RF transceiver, baseband, and protocol stack. The system offers services that enable the connection of devices and the exchange of a variety of data classes between these devices.

The *Bluetooth* RF (physical layer) operates in the unlicensed ISM band at 2.4GHz. The system employs a frequency hop transceiver to combat interference and fading, and provides many FHSS carriers. RF operation uses a shaped, binary frequency modulation to minimize transceiver complexity. The symbol rate is 1 Megasymbol per second (Msps) supporting the bit rate of 1 Megabit per second (Mbps) or, with Enhanced Data Rate, a gross air bit rate of 2 or 3Mb/s. These modes are known as Basic Rate and Enhanced Data Rate respectively.

During typical operation, a physical radio channel is shared by a group of devices that are synchronized to a common clock and frequency-hopping pattern. One device provides the synchronization reference and is known as the master. All other devices are known as slaves. A group of devices synchronized in this fashion form a piconet. This is the fundamental form of communication for *Bluetooth* wireless technology.

Devices in a piconet use a specific frequency-hopping pattern that is algorithmically determined by certain fields in the *Bluetooth* specification address and clock of the master. The basic hopping pattern is a pseudo-random ordering of the 79 frequencies in the ISM band. The hopping pattern may be adapted to exclude a portion of the frequencies that are used by interfering devices. The adaptive hopping technique improves *Bluetooth* technology co-existence with static (non-hopping) ISM systems when these are co-located.

The physical channel is sub-divided into time units known as slots. Data is transmitted between *Bluetooth* enabled devices in packets that are positioned in these slots. When circumstances permit, a number of consecutive slots may be allocated to a single packet. Frequency hopping takes place between the transmission and reception of packets. *Bluetooth* technology provides the effect of full duplex transmission through the use of a time-division duplex (TDD) scheme.

Above the physical channel there is a layering of links and channels and associated control protocols. The hierarchy of channels and links from the physical channel upwards is physical channel, physical link, logical transport, logical link and L2CAP channel.

Within a physical channel, a physical link is formed between any two devices that transmit packets in either direction between them. In a piconet physical channel there are restrictions on which devices may form a physical link. There is a physical link between each slave and the master. Physical links are not formed directly between the slaves in a piconet.

The physical link is used as a transport for one or more logical links that support unicast synchronous, asynchronous and isochronous traffic, and broadcast traffic. Traffic on logical links is multiplexed onto the physical link by occupying slots assigned by a scheduling function in the resource manager.

A control protocol for the baseband and physical layers is carried over logical links in addition to user data. This is the link manager protocol (LMP). Devices that are active in a piconet have a default asynchronous connection-oriented logical transport that is used to transport the LMP protocol signaling. For historical reasons this is known as the ACL logical transport. The default ACL logical transport is the one that is created whenever a device joins a piconet. Additional logical transports may be created to transport synchronous data streams when this is required.

The link manager function uses LMP to control the operation of devices in the piconet and provide services to manage the lower architectural layers (radio layer and baseband layer). The LMP protocol is only carried on the default ACL logical transport and the default broadcast logical transport.

Above the baseband layer the L2CAP layer provides a channel-based abstraction to applications and services. It carries out segmentation and reassembly of application data and multiplexing and de-multiplexing of multiple channels over a shared logical link. L2CAP has a protocol control channel that is carried over the default ACL logical transport. Application data submitted to the L2CAP protocol may be carried on any logical link that supports the L2CAP protocol.

### D. IEEE 802.16

The IEEE 802.16[13] is a standard for wireless metropolitan area networks (MAN) and provides network access to buildings through exterior antennas communicating with central radio base stations (BSs). The wireless MAN offers an alternative to cabled access networks, such as fiber optic links, coaxial systems using cable modems, and digital subscriber line (DSL) links. The current IEEE 802.16 standard require users inside the building to connect it with conventional in-building networks such as, for data, Ethernet (IEEE Standard 802.3) or wireless LANs (IEEE Standard 802.11). However, the fundamental design of the standard may eventually allow for the efficient extension of the Wireless MAN networking protocols directly to the individual user. Hence, the IEEE 802.16 has potential to reduce the cabling for large complex systems or even the cabling among facilities on the Moon's surface.

The IEEE 802.16 Standard was designed to evolve as a set of air interfaces based on a common MAC protocol but with physical layer specifications dependent on the spectrum of use and the associated regulations. The standard, approved in 2001, addresses frequencies from 10 to 66 GHz, where extensive spectrum is currently available worldwide but at which the short wavelengths introduce significant deployment challenges. An amendment of the standard denoted IEEE 802.16a extends the air interface support to lower frequencies in the 2–11 GHz band, including both licensed and license exempt spectra. Compared to the higher frequencies, such spectra offer the opportunity to reach many more customers less expensively, although at generally lower data rates.

The PHY layer of the IEEE 802.16 uses burst single-carrier modulation with adaptive burst profiling in which transmission parameters, including the modulation and coding schemes, may be adjusted individually to each subscriber station (SS) on a frame-by-frame basis. The standard also allows duplex communication between the BS and SS. Both Time Division Duplexing (TDD) and burst Frequency Division Duplexing (FDD) variants are defined. The bandwidth of each channel is 20 or 25 MHz (typical U.S. allocation) or 28 MHz (typical European allocation). Randomization is performed for spectral shaping and to ensure bit transitions for clock recovery.

In the Medium Access Control (MAC) layer, the IEEE 802.16 Standard defines two general service-specific convergence sub-layers for mapping services to and from 802.16 MAC connections. The ATM convergence sub-layer is defined for ATM services, and the packet convergence sub-layer is defined for mapping packet services such as IPv4, IPv6, Ethernet, and virtual local area network (VLAN). The primary task of the sub-layer is to classify service data units (SDUs) to the proper MAC connection, preserve or enable quality of service (QoS), and enable bandwidth allocation. The mapping takes various forms depending on the type of service. In addition to these basic functions, the convergence sub-layers can also perform more sophisticated functions such as payload header suppression and reconstruction to enhance airlink efficiency.

In general, the IEEE 802.16 MAC is designed to support a point-to-multipoint architecture with a central BS handling multiple independent sectors simultaneously. On the downlink, data to SSs are multiplexed in time division multiplex (TDM) fashion. The uplink is shared between SSs in time division multiple access (TDMA) fashion.

The 802.16 MAC is connection-oriented. All services, including inherently connectionless services, are mapped to a connection. This provides a mechanism for requesting bandwidth, associating QoS and traffic parameters, transporting and routing data to the appropriate convergence sub-layer, and all other actions associated with the contractual terms of the service. Connections are referenced with 16-bit connection identifiers (CIDs) and may require continuously granted bandwidth or bandwidth on demand.

Each SS has a standard 48-bit MAC address, but this serves mainly as an equipment identifier, since the primary addresses used during operation are the CIDs. Upon entering the network, the SS is assigned three management connections in each communication direction. These three connections reflect the three different QoS requirements used by different management levels. The first of these is the basic connection, which is used for the transfer of short, time-critical MAC and radio link control (RLC) messages. The primary management connection is used to transfer longer, more delay-tolerant messages such as those used for authentication and connection setup. The secondary management connection is used for the transfer of standards-based management messages such as Dynamic Host Configuration Protocol (DHCP), Trivial File Transfer Protocol (TFTP), and Simple Network Management Protocol (SNMP). In addition to these management connections, SSs are allocated transport connections for the contracted services. Transport connections are unidirectional to facilitate different uplink and downlink QoS and traffic parameters; they are typically assigned to services in pairs.

The MAC reserves additional connections for other purposes. One connection is reserved for contention-based initial access. Another is reserved for broadcast transmissions in the downlink as well as for signaling broadcast contention-based polling of SS bandwidth needs. Additional connections are reserved for multicast, rather than broadcast, contention-based polling. SSs may be instructed to join multicast polling groups associated with these multicast polling connections.

## IV. Summary of Sensor Cable Reduction Techniques

Four classes of sensor cable reduction techniques have been surveyed in the first part of this paper. These techniques are power line communication, serial sensor buses, compound serial buses, and wireless network. The power line communication approach uses the power line to carry both power and data, so that the conventional data lines can be eliminated. The serial sensor bus approach reduces most of the cabling by connecting all the sensors with a single (or redundant) serial bus. Many standard buses for industrial control and sensor buses can support several hundreds of nodes, however, have not been space qualified. Conventional avionics serial buses such as the Mil-Std-1553B bus and IEEE 1394a are space qualified but can support only a limited number of nodes. The third approach is to combine avionics buses to increase their addressability. The wireless networks can eliminate all the cable mass but their reliability, EMI/EMC, and flight qualification issues have to be addressed. The survey is not exhaustive but only intended to point out directions for future researches. In the second part of the paper, the techniques to optimize sensor placement to reduce cable mass will be discussed.

## V. Sensor Optimization and Evaluation for Massive Space Data Collection

One of the major challenges of future space exploration programs is to process a huge volume of data collected from a large number of sensors. Such a large system of sensors poses two challenging problems: (1) handling the design issues of integrating the sensors in the system; (2) processing the huge data collected by the sensors. In the design level, the conventional avionics system design of a large system of sensors leads to a large mass of cabling and unacceptable weight. The wireless technology approach suggested in this paper tackles this problem. On the other hand, utilizing and interpreting large volumes of data is problematic under routine conditions. To identify causes of anomalies, an effort should be undertaken to analyze large volumes of data. A new technology developed at JPL is described to tackle these challenging problems for design analysis and optimal selection of sensors to maximize diagnosability of the system while minimizing the cost of sensors deployment. This technology is capable also of performing sensor validation. For this purpose, we utilize the structure of the system to determine the source of an observed discrepancy: is it a faulty component or a faulty sensor. The result is a drastic reduction in the number of false alarms. This methodology can, on one hand, optimize the number of sensors while maximizing the diagnosability of the system, and, on the other hand, by analyzing the system of sensors, consolidates many sensor readings into a few indicators to reduce the space of data to a manageable size.Diagnostic/prognostic capability of any system depends on how well the sensors cover the space of possible faults. Having extra sensors on a space vehicle adds to weight, cost, size of the data space, and potential points of failure, and might not directly improve diagnostic/prognostic capability of the system. There is a need for careful optimization and verification of the system design to trade off the conflicting requirements. Current approaches to sensor selection are *ad hoc* and cannot be systematically applied to many systems of interest. The key innovation of our new approach is to develop a new mathematical formulation of the problem and to develop efficient algorithms that can handle large systems of interest. To our knowledge, this is the first systematic formulation and solution for optimal sensor selection problem. The method can be used both at the design level where the number and position of sensors need to be determined and for the case where sensors are added to a legacy system to enhance its diagnosability.

The quality and efficiency of a diagnosis system depends on the availability and relevance of the information it can retrieve. The quality of the measurements is expressed by the *diagnosability degree,* i.e., given a set of sensors, which faults can be discriminated? There is no straightforward relation between the number of sensors and diagnosability of the systems; increasing the number of sensors alone does not guarantee a higher level of diagnosability. The relevance of information provided by an additional sensor and its correlation with information provided by other sensors must also be taken into account. Besides the issue of diagnosability, we should also consider the economical issues, that is, we must provide a sensor system that achieves a desired degree of diagnosability at the lowest possible cost of sensors deployment. The different issues regarding sensor selection problem can be summarized as follows.

- *Diagnosability Degree.* Determining the diagnosability degree of a system, i.e., characterizing the set of the faults that can be discriminated.
- *Minimal Sensor Set.* Finding a minimal additional sensor set that guarantees a specific degree of diagnosability.
- *Minimal Cost Sensors.* In the case that different sensors are assigned with different costs, finding the minimal cost additional sensors that achieve a specific degree of diagnosability.

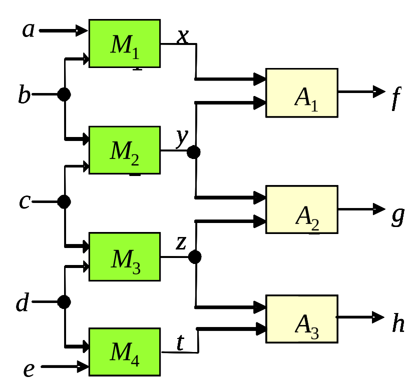


**Figure 10. An adder-multiplier**

Our new approach for solving these problems is motivated by our successful method for solving the diagnosis problem.[14] The structural analysis of the system and the potential information carried by each sensor provide a set of relations usually called the *Analytical Redundant Relations* (ARRs).[15] We can also consider additional sensors (the potential sensors that will provide the desired degree of diagnosability) and their corresponding ARRs. The information of all these ARRs can be summarized in a *fault signature matrix*. Then the above sensor optimization problem can be formulated as combinatorial problem regarding the signature matrix. The existing methods for solving this combinatorial problem usually boil down to exhaustive search methods.[16,17] We present a novel mapping of the above sensor optimization problem as a special case of 0-1 Integer Programming problem. We then propose a new and powerful branch-and-bound technique for this problem. Our new approach relies on our recent algorithmic advances for solving the model-based diagnosis problem[14]. For solving the diagnosis problem, we have found a new branch-and-bound technique that has achieved an order of magnitude speedup over the standard algorithms.[18] Combination of a new branch-and-bound technique and the signature matrix approach provides a powerful efficient technique for solving the difficult problem of sensor selection optimization.

## A. Signature Matrix

In the model-based approach, the behavior of a system is described by a set of relations among variables (parameters) of the system. These relations, not only describe the nominal behavior of each component, but they also determine the structure and interconnections of the components. A simple example explains this notion. Consider the circuit represented in Figure 10 (this is an example of a *polybox system*[15]). This system consists of 7 components, which are 4 multiplier gates, $M_1$, $M_2$, $M_3$, and $M_4$ and 3 adder gates, $A_1$, $A_2$, and $A_3$. Let $x$, $y$, $z$, and $t$ denote the outputs of the multiplier gates and $f$, $g$, and $h$ denote the outputs of the adder gates. The model of this system can be described by the following relations: Component $M_1$ $r_1$: $x = a \times b$, Component $M_2$ $r_2$: $y = b \times c$, Component $M_3$ $r_3$: $z = c \times d$, Component $M_4$ $r_4$: $t = d \times e$, Component $A_1$ $r_5$: $f = x + y$, Component $A_2$ $r_6$: $g = y + z$, Component $A_3$ $r_7$: $h = z + t$. We call these relations the *primary relations* (PRs) of the system and we define the set the *variables* of the system as $V = \{x, y, z, t, f, g, h\}$.

Once the sensors are introduced, the set of variables $V$ can be partitioned as $V = O \cup U$, where $O$ is the set of observed variables (i.e., variables measured by the sensors) and $U$ the set of unknown (non-measured) variables. If the number of relations in $E$ is more than the number of unknown variables $U$, then it is possible to find relations among observed variables $O$. These relations are called *Analytical Redundant Relations* (ARRs). The basic property of an ARR is that it can be evaluated from the observed values. We consider a set $\mathbf{F}$ of faults. In most cases, each fault $F \in \mathbf{F}$ is identified by a malfunction of a set of components $C_1, \ldots, C_t$ and is denoted as $F_{C_1,\ldots,C_t}$. The *Fault Signature Matrix*, or simply the Signature Matrix, is a 0/1 matrix where the rows are labeled by ARRs and columns are labeled by the faults, such that for the entry $s_{ij}$, at row labeled by the ARR $R_i$ and the column labeled by the fault $F_j$, we have $s_{ij}$=1 if a component involved in the fault $F_j$ appears in $R_i$, otherwise $s_{ij} = 0$. Therefore, each column of signature matrix is a binary *Fault Signature Vector* (FSV) containing 1 for each ARR sensitive to that fault and 0 for insensitive relations.

One obvious way to achieve maximum discriminability is to measure all the variables of the system. However, it may be possible to achieve the same level of discriminability by measuring a subset of all variables. Therefore, the problem of finding the optimal sensors is equivalent to finding minimal number of additional sensors that provide the same level of discriminability as the case where every variable is measured. This is done by assuming that all unknown variables of the system have a hypothetical sensor and the corresponding (hypothetical) ARRs are considered. The new signature matrix that is obtained is called the *Hypothetical Signature Matrix* (HSM). For example, in the case of the system of Figure 1, to generate the hypothetical signature matrix (HSM), we assume that all variables $x$, $y$, $z$, $t$, $f$, $g$, and $h$ are observed. Table 3 shows the corresponding HSM and also the associated ARRs.

**Table 3. The Hypothetical Signature Matrix (HSM) of the system of Figure 10**

| No. | ARR | $M_1$ | $M_2$ | $M_3$ | $M_4$ | $A_1$ | $A_2$ | $A_3$ |
|---|---|---|---|---|---|---|---|---|
| 1 | $x-ab=0$ | 1 | 0 | 0 | 0 | 0 | 0 | 0 |
| 2 | $y-bc=0$ | 0 | 1 | 0 | 0 | 0 | 0 | 0 |
| 3 | $z-cd=0$ | 0 | 0 | 1 | 0 | 0 | 0 | 0 |
| 4 | $t-de=0$ | 0 | 0 | 0 | 1 | 0 | 0 | 0 |
| 5 | $f-x-y=0$ | 0 | 0 | 0 | 0 | 1 | 0 | 0 |
| 6 | $g-y-z=0$ | 0 | 0 | 0 | 0 | 0 | 1 | 0 |
| 7 | $h-z-t=0$ | 0 | 0 | 0 | 0 | 0 | 0 | 1 |
| 8 | $f-g-x+z=0$ | 0 | 0 | 0 | 0 | 1 | 1 | 0 |
| 9 | $g-h-y+t=0$ | 0 | 0 | 0 | 0 | 0 | 1 | 1 |
| 10 | $f-ab-bc=0$ | 1 | 1 | 0 | 0 | 1 | 0 | 0 |
| 11 | $g-bc-cd=0$ | 0 | 1 | 1 | 0 | 0 | 1 | 0 |
| 12 | $h-cd-de=0$ | 0 | 0 | 1 | 1 | 0 | 0 | 1 |
| 13 | $f-g-ab+cd=0$ | 1 | 0 | 1 | 0 | 1 | 1 | 0 |
| 14 | $g-h-bc+de=0$ | 0 | 1 | 0 | 1 | 0 | 1 | 1 |
| 15 | $f-ab-y=0$ | 1 | 0 | 0 | 0 | 1 | 0 | 0 |
| 16 | $g-bc-z=0$ | 0 | 1 | 0 | 0 | 0 | 1 | 0 |
| 17 | $h-cd-t=0$ | 0 | 0 | 1 | 0 | 0 | 0 | 1 |
| 18 | $f-x-bc=0$ | 0 | 1 | 0 | 0 | 1 | 0 | 0 |
| 19 | $g-y-cd=0$ | 0 | 0 | 1 | 0 | 0 | 1 | 0 |
| 20 | $h-z-de=0$ | 0 | 0 | 0 | 1 | 0 | 0 | 1 |

| | | | | | | | | |
|---|---|---|---|---|---|---|---|---|
| 21 | $f – g – ab + z = 0$ | 1 | 0 | 0 | 0 | 1 | 1 | 0 |
| 22 | $g – h – bc + t = 0$ | 0 | 1 | 0 | 0 | 0 | 1 | 1 |
| 23 | $f – g – x + cd = 0$ | 0 | 0 | 1 | 0 | 1 | 1 | 0 |
| 24 | $g – h – y + de = 0$ | 0 | 0 | 0 | 1 | 0 | 1 | 1 |
| 25 | $f – g + h – x – t = 0$ | 0 | 0 | 0 | 0 | 1 | 1 | 1 |
| 26 | $f – g + h – ab\ t = 0$ | 1 | 0 | 0 | 0 | 1 | 1 | 1 |
| 27 | $f – g + h – x – de = 0$ | 0 | 0 | 0 | 1 | 1 | 1 | 1 |
| 28 | $f – g + h – ab – de = 0$ | 1 | 0 | 0 | 1 | 1 | 1 | 1 |

The set of sensors corresponded with each ARR (rows of Table 3) are as follows, respectively:

{*x*}, {*y*}, {*z*}, {*t*}, {*x, y, f*}, {*y, z, g*}, {*z, t, h*}, {*x, z, f, g*}, {*y, t, g, h*}, {*f*}, {*g*}, {*h*}, {*f, g*}, {*g, h*}, {*y, f*}, {*z, g*}, {*t, h*}, {*x, f*}, {*y, g*}, {*z, h*}, {*z, f, g*}, {*t, g, h*}, {*x, f, g*}, {*y, g, h*}, {*x, t, f, g, h*}, {*t, f, g, h*}, {*x, f, g, h*}, {*f, g, h*}.

### B. Integer Programming Formulation

To describe the mapping of the Sensor Selection Optimization Problem as an *integer-programming* problem, let us consider a signature matrix *H* of a system. Let $M=H^T$, i.e., the $n \times m$ matrix *M* is the transposed of *H*. For every row *R* of *H*, or equivalently every column *C* of *M*, a corresponding set of sensors $\mathsf{S}(R)$ or $\mathsf{S}(C)$ is defined. Then an equivalent formulation of the problem is as follows: choose a subset of the columns of *M* such that the submatrix defined by these columns has no zero rows, all its rows are distinct, and the total number of corresponding sensors is minimal. Let us define a *binary* vector $\boldsymbol{x} = (x_1, x_2, \ldots, x_m)$ whose dimension is the same as the number of columns of the matrix *M*. Then we can interpret $\boldsymbol{x}$ as a selection of a subset of columns of *M*: $x_j=1$ if and only if the $j^{\text{th}}$ column of *M* is chosen. Then the condition $M\,\boldsymbol{x} \geq \mathbf{1}$ (where $\mathbf{1}=(1,1,\ldots,1)^T$ is an all-one vector of appropriate dimension) implies that the solution defined by $\boldsymbol{x}$ has this property that the corresponding submatrix has no all-zero row. To satisfy the other condition, let us define the matrix $M_2$ with $n(n–1)/2$ rows and *m* columns as follow: each row $R_{i,j}$ of $M_2$ is associated with a (distinct) pair $R_i$ and $R_j$ of rows of *M*, and $R_{i,j}=|\,R_i - R_j\,|$; i.e., $k^{\text{th}}$ entry of $R_{i,j}$ is equal to 1 if $k^{\text{th}}$ entries of $R_i$ and $R_j$ are distinct, otherwise it is equal to 0 (in another word, if we consider these vectors as Boolean vectors, then $R_{i,j}= R_i \oplus R_j$, where $\oplus$ denotes the Boolean exclusive-OR operation). Then the condition $M_2\,\boldsymbol{x} \geq \mathbf{1}$ implies that the solution defined by $\boldsymbol{x}$ has this property that all rows of the corresponding submatrix are distinct. So if we consider the matrix.

$$\tilde{M} = \begin{pmatrix} M \\ M_2 \end{pmatrix},$$

then the Sensor Selection Optimization Problem can be formulated as the following optimization problem:

$$\textit{minimize}\ \left|\bigcup_{i=1}^{m} \mathsf{S}(x_i)\right|,$$

$$\textit{subject to}\ \tilde{M}\boldsymbol{x} \geq \mathbf{1}, \quad x_j = 0 \text{ or } 1.$$

Here $\mathsf{S}(x_i)$ is the set of sensors associated with the $i^{\text{th}}$ column of *M* if $x_i=1$, and it is empty set if $x_i=0$.

Utilizing this integer programming formulation, we were able to calculate lower and upper bounds for the problem and use them to implement a powerful branch-and-bound method for solving this problem.[18]

### C. Validation and Benchmarking

To validate this new algorithm, we generated a *Mathematica* code based on it, and compared its results with results of an exhaustive search algorithm that guarantees correct solution. We ran both algorithms for hundreds of test cases. In all cases, the results of both algorithms were the same.

**Table 4. Comparison of performance of the new algorithm with the exhaustive search algorithm (in each case the results are based on 100 random signature matrices)**

| Size | New Algorithm | | Exhaustive Search Algorithm |
|---|---|---|---|
| | Average search tree size | Max search tree size | Search tree size |
| 15×12 | 3.16 | 20 | $> 3\times10^{5}$ |
| 23×18 | 6.4 | 44 | $> 8\times10^{6}$ |
| 31×24 | 64.14 | 424 | $> 2\times10^{9}$ |
| 41×32 | 131.02 | 466 | $> 2\times10^{12}$ |
| 53×42 | 392.44 | 1220 | $> 9\times10^{15}$ |
| 61×48 | 418.92 | 1316 | $> 2\times10^{18}$ |
| 67×53 | 344.4 | 810 | $> 10^{20}$ |
| 73×58 | 397.48 | 998 | $> 9\times10^{21}$ |

To evaluate the performance of the new algorithm, we performed the following experiment.

For odd values of $j = 7, \ldots, 75$, we considered matrices of dimension $j \times \left(j - \lceil j/5 \rceil\right)$ and for each such dimension we generated 100 random signature matrices with corresponding sets of sensors, where each sensor set is chosen randomly of size at most 4 from a set of at most 9 sensors.

For each dimension, the average size of the search tree and also the maximum and minimum of these trees, among the 100 random cases, are recorded.

The reason we gathered information regarding the search tree is that the size of search tree is the main parameter that determines the efficiency of the algorithm; i.e., it determines both time and memory the algorithm utilizes. Also this size only depends on the algorithm neither the programming language used to code the algorithm nor the machine used to run the code. As a comparison, note that an exhaustive search algorithm for a case with *m* rows requires a search tree whose size is in order of $2^m$. To provide a better picture of this phenomenon, in Table 4 we have compared the results of performance of our algorithm with the exhaustive search algorithm for some sample dimensions.

## VI. Applications:

The Exploration Systems & Technology Office (ESTO) has outlined a path for JPL to the Constellation Program (CxP). What is unique about wireless technology is its applicability to avionics in NASA Exploration Systems Mission Directorate (ESMD) program offices: JSC – Constellation Program and MSFC – Lunar Precursor and Robotic Program (LPRP). Wireless avionics will not replace all of the critical hard wired functions on a space vehicles, it provides a robust, low mass, inherently redundant enabling technology for space exploration. Cables for power distribution, safe/arm pyro events are still required. Advances in high-speed hard-wired bus technology would be used in conjunction with wireless avionics.

The present need for the Space Interferometry Mission (SIM) to reduce its overall mass presents an opportunity to find new ways to transfer science and engineering data. Near term wireless avionics architecture for the SIM project lays a foundation for the next generation of architectures with faster data rates and greater reliability regarding the mitigation of multipath interference of wireless signals. The next generation space suits, CLV, CEV, CaLV, EDS and Lunar Surface Access Module (LSAM) are likely candidates for advances in local area wireless networks. Hundreds of channels of State-Of-Health (SOH) data are exchanged between astronauts, spacecrafts and lunar vehicles. In this advanced architecture, the implementation of Fault Detection, Diagnosis and Remediation (FDDR) is taken to new levels of reliability where any node in the wireless network can monitor the SOH of any other node and take corrective action if there is a problem.

The CEV “Smart Buyer” team provides the expertise in the evaluation of wireless protocols which meet the range, data rate, power and quantity of nodes for space applications. Key characteristics of the wireless network are simultaneous communications between multiple nodes without multiple path or crosstalk interference. High data rate HDTV as well as low data rate SOH telemetry must be merged into a wireless space protocol standard. To achieve this goal various commercial industry standards must be evaluated before selecting one industry standard to be modified for space applications.

## VII. Summary

This paper has provided a survey of technologies that are potentially capable to reduce cabling for NASA’s Constellation Program (including CEV, CLV, and unmanned space systems). The technologies surveyed include power line communication such as LonWorks and HomePlug, serial sensor buses such as FieldBuses and IEEE 1451, compound serial buses such as JPL’s IEEE 1394A/Mil-Std-1553B architecture, wireless networks such as the IEEE 802.15.3A, IEEE 802.11 family, Bluetooth, and IEEE 802.16. A graphic comparison of the performance of these techniques verses the needs of typical applications is shown in Figure 11.

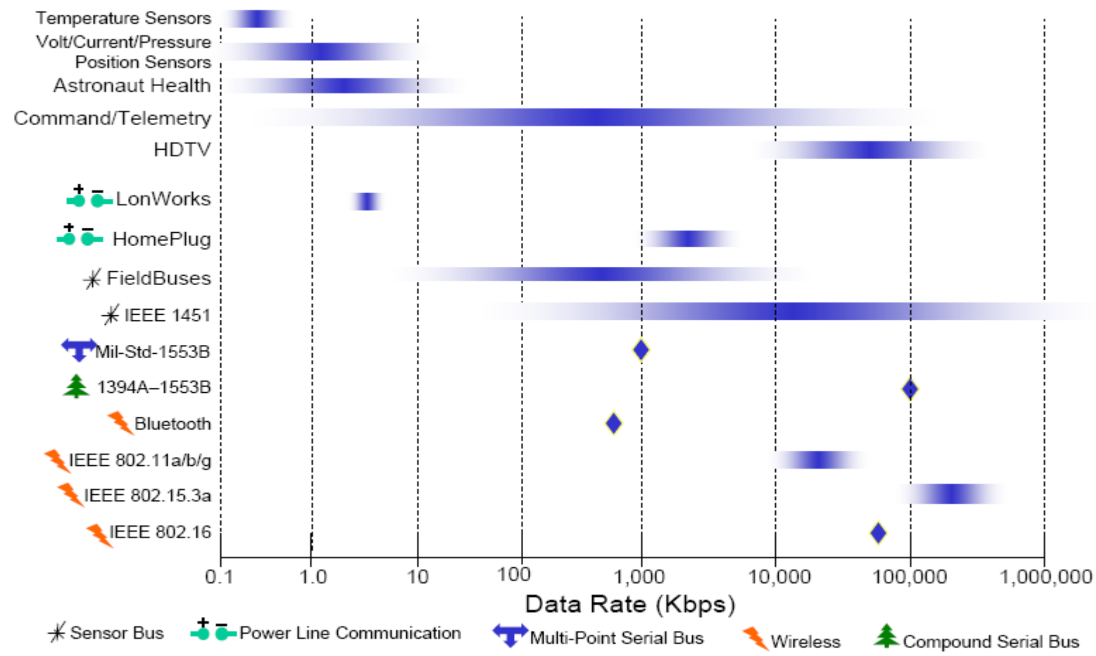


**Figure 11. Comparison of Surveyed Cable Reduction Techniques**

While this list is not exhaustive, it provides some directions for future trade-off studies and points out the required areas of development for space application of these technologies. It has also presented new approaches to sensor placement optimization with regard to with regard to diagnosability, cost and validation.

We have also presented a new method for solving the optimal sensor selection problem. The method discussed here mainly concerns with the basic case of finding minimal size set of sensor among all possible (hypothetical) sensors. But this does not restrict the capability of our method to deal with other scenarios for sensor selection. For example, in the case that there is a *cost* or *weight* associated with each sensor, the optimization problem is to find the set of *minimal cost (weight)* sensors. Our technique can easily be modified to cover this case as well. For this purpose, we have to modify the subroutine that finds the upper bound such that instead of the size of the set of sensors the total cost of the sensors is considered as the objective function. Also in the case that there is already a fixed set of sensors and we want to add more sensors to the system to enhance its diagnosability, we can simply utilize our method but instead of the hypothetical signature matrix we have to consider its submatrix obtained by deleting the rows corresponding with the set of fixed sensors. Our method is also capable of handling other related issues, such as analyzing sensor redundancy and sensitivity, sensor validation for reducing false alarm and study of impact of sensor failure. In the subsequent paper we will discuss all this matters in detail.

## Acknowledgment

The research described in this paper was carried out by the Jet Propulsion Laboratory, California Institute of Technology, under a contract with the National Aeronautics and Space Administration.

## References

[1] Echelon Corporation, *Introduction to LonWorks System*, 1999

[2] M. Lee, R. Newman, H. Latchman, S. Katar and L. Yonge, “HomePlug 1.0 powerline communication LANs – protocol description and performance results,” *Int. J. Commun. Syst.* 2003

[3] Echelon Corporation, *LonWorks PLT-22 Power Line Transceiver User’s Guide (110 kHz – 140 kHz Operation) Version 1.2*, 2002

[4] Smart Technology Assistance Center Web Site
http://www.tyco-stac.com/network_solutions/overview_network_comm.html

[5] IEEE Standard Association web site
http://grouper.ieee.org/groups/1451/0/body%20frame_files/Family-of-1451_handout.htm

[6] IEEE, *1451.3™ IEEE Standard for a Smart Transducer Interface for Sensors and Actuators—Digital Communication and Transducer Electronic Data Sheet (TEDS) Formats for Distributed Multidrop Systems*, 2003
[7] A. Tai, S. Chau, L. Alkalai, "COTS-based fault tolerance in deep space: A case study on IEEE 1394 application," *International Journal of Reliability, Quality and Safety Engineering*, vol. 8, Sept. 2000.
[8] NOAA News On-Line (Story 2280), http://www.noaanews.noaa.gov/stories2004/s2280.htm
[9] Ketan Mandke, Haewoon Nam, Lasya Yerramneni, Christian Zuniga and Ted Rappaport, "The Evolution of Ultra Wide Band Radio for Wireless Personal Area Networks," *High Frequency Electronics*, September 2003
[10] Liuqing Yang, and Georgios B. Giannakis, "Multistage Block-Spreading for Impulse Radio Multiple Access Through ISI Channels," *IEEE Journal on Selected Areas in Communications*, Vol. 20, No. 9, December 2002.
[11] IEEE Standard 802.11-1997
[12] Bluetooth Consortium web site http://www.bluetooth.com/Bluetooth/Learn/Works/
[13] Carl Eklund, Roger Marks, Kenneth Stanwood and Stanley Wang, "IEEE Standard 802.16: A Technical Overview of the WirelessMAN™ Air Interface for Broadband Wireless Access," I*EEE Communications Magazine*, June 2002
[14] Fijany and F. Vatan, New high performance algorithmic solution for diagnosis problem, *Proceedings of 2005 IEEE Aerospace Conference*, March 2005.
[15] M-O. Cordier, P. Dague, F. Levy, J. Montmain, M. Staroswiecki, and L. Travé-Massuyès, Conflicts versus analytical redundancy relations: a comparative analysis of the model based diagnosis approach from the artificial intelligence and automatic control perspectives, *IEEE Transactions on Systems, Man, & Cybernetics, Part B: Cybernetics*, Vol. 34, No. 5, pp. 2163–2177, Oct. 2004.
[16] S. Spanache and T. Escobet, Fault diagnosability: a component-oriented approach, *Proceedings of Workshop on Identification, Optimization, and Control of Hybrid System*, Valencia, Spain, January 2004.
[17] L. Travé-Massuyès, T. Escobet and R. Milne, Model-based Diagnosability and sensor placement application to a frame 6 gas turbine subsystem, *Proceedings of IJCAI*, pp. 551–556, 2001.
[18] A. Fijany and F. Vatan, A New Efficient Algorithm for Analyzing and Optimizing the System of Sensors, *2006 IEEE Aerospace Conference*, March 2006.